Management power of renewable energy in multiple sources system to feeding the rotor of a doubly-fed induction generator

Kendzi Mohammed[1], Aissaoui Abdelghani[1], Younes Dris[2], Bouiri Abdesselam[3], Haddar Mabrouk[3]
[1]Department of Electrical Engineering, Tahri Mohammed Bechar University, Bechar, Algeria
[2]Department of Electrical Engineering, Tlemcen University, Tlemcen, Algeria
[3]Laboratory of Smart Grids and Renewable Energies (S.G.R.E), Department of Electrical Engineering, University of Tahri Mohamed Bechar, Bechar, Algeria

Article Info

Article history:

Received Apr 2, 2022
Revised Jul 6, 2022
Accepted Sep 5, 2022

Keywords:

Battery
Photovoltaic systems
Sliding mode
Supervisory control
Wind energy

ABSTRACT

The purpose of this paper is the elimination of interruptions of electrical energy produced by a multi-source production system, so we have assured the feed of DFIG rotor in a wind system by different energy sources (photovoltaic generator, battery group) and switchover between them by auxiliary contacts controlled by a supervisor via a power control algorithm. For the photovoltaic generator, a controller for tracking the maximum power point is designed using direct search approach perturb & observe method. For the battery group, the installation of a number of the capacitor battery elements in series and in parallel will be kept the power necessary to supply the DFIG rotor. For the wind system, it contains the power generated by DFIG is controlled by sliding mode system. With regard to switching between electrical energy sources, our proposed system relies on an algorithm to compare the energies produced by each generator with the energy required to feed the DFIG rotor and the energies consumed in the system, where the energy source with high production energy and available is exploited to feed the system and charge the batteries. Simulations were performed to confirm the reliability and efficacy of the system proposed.

Corresponding Author:

Kendzi Mohammed
Department of Electrical Engineering, Tahri Mohammed Bechar University
Bechar, B.P 417 Bechar 08000, Algeria
Email: kendzimohammed@gmail.com

1. INTRODUCTION

Hybrid systems renewable energies (HRES) are becoming popular in the typologies of renewable energy. A HRES is composed of two or more renewable energy sources with appropriate energy conversion technology connected together to feed power to the local load or grid, where the researchers cared to combine the wind power and PV because they are the most promising technologies for supplying load in remote and rural regions with strengthening the hybrid system with a storage system. In last years, recent researches have been developed in the area of hybrid system. Azzaoui *et al*. [1] have focused on increasing the cost-effectiveness of control methods through the rapid adjustment of the parameters of system where was control the systems by the backstepping method and [2] to control the PV-wind hybrid system connected to grid by using sliding mode, and [3] also did control of the photoelectric generator for used in feeding of the independent wind turbine system by fuzzy logic method.

However, these models still complain of negative factors, which are: interruption of production caused by the absence of sunlight and interruption of production due to the absence of feeding the rotor through the grid when using the double feed generator. For this, the researchers study the field of achieving integrated feeding within a single system while ensuring energy storage where was done combined the control of doubly-fed induction generator (DFIG-based) wind turbine and battery energy storage system [4], improve the power quality and capacity of a battery-powered and solar-wind hybrid power system [5], and control of the photoelectric generator for used in feeding of the independent wind turbine system [3]. With the multiplicity of production systems used in the one hybrid system, researchers had to develop a management system that saves energy according to priorities, as they relied on a management system based on proportional integral (PI) controller [6].

In this context, we proposed a new management system based on the sliding mode to control the power generated by the double feed generator and algorithm of the control system with the supervisor of the different production powers. So, our goal is to develop a hybrid system (wind/photovoltaic/battery group) which can ensure an uninterrupted power generation. A maximum power is extracted from the wind and PV group. The wind turbine used is based on a doubly-fed induction generator DFIG. The power generated by the wind turbine is injected directly to the grid. The PV power is used to supply the rotor of DFIG and to charge the battery group; the rest of this power is injected to the grid. The purpose of the use of the capacitor bank group is to ensure the rotor supply of the DFIG in the case of lack of photovoltaic energy and in the case of failure of the photovoltaic system. With the help of a supervisor, this system can manage the transfer of these powers to all destinations to ensure the continuity of the service.

The rest of the paper is organized in 9 sections. The second section presents the hybrid system (photovoltaic/wind/battery group). The third section is devoted to modelling the components of the wind turbine. In the fourth section, the control strategy of the DFIG is described, and the technique of sliding mode control is applied to control the active and reactive powers generated by the wind turbine. The fifth section describes the photovoltaic conversion chains, and gives the model of its different parts with the control methodology used. The sixth section presents the perturb & observe (P&O) control algorithm for tracking the maximum power delivered by the photovoltaic generator. In the seventh section, a modelling of the battery group is established. The eighth section is devoted to the strategy designed to manage the generated electrical energy by all the system. The simulation results are discussed and analysed in the ninth section. In the last section, conclusions are summarized.

2. THE PHOTOVOLTAIC/WIND SYSTEM

The hybrid system contains two sources of renewable energies; the first source is a 7.5 kW rated power wind turbine with DFIG directly connected to the power grid. The power generated by the DFIG is controlled by sliding mode control technique. The second source is solar energy; it is equipped with a photovoltaic conversion system; the rated power of this system is 6.8 kW. This power is used to feed the rotor of the DFIG, to charge the group of batteries and the rest is injected to the grid. The power generated by the hybrid system is managed as shown in Figure 1.

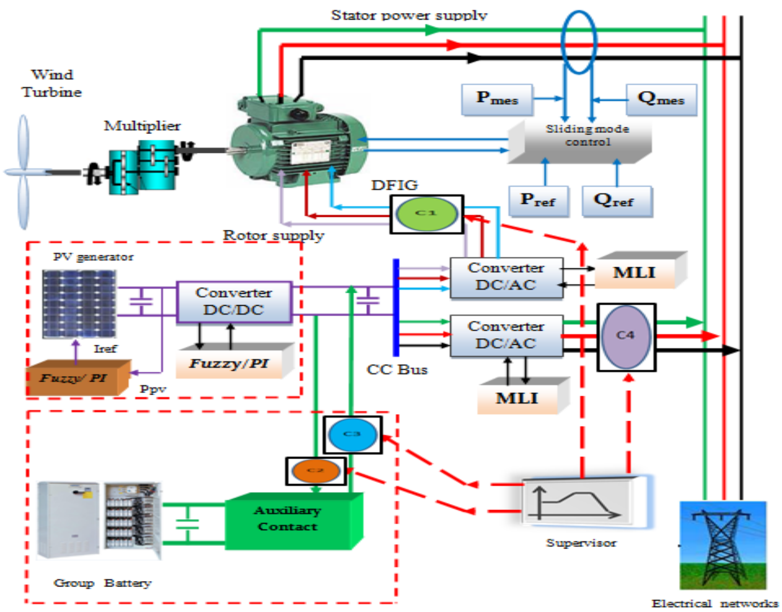

Figure 1. The considered hybrid system

3. THE MATHEMATICAL MODEL OF THE WIND TURBINE

3.1. Modeling of the turbine

The mathematical model of aeroturbine is [7], [8]:

$$J\frac{d}{dt}\Omega_{mec} = C_g - C_{em} - f\,\Omega_{mec} \tag{1}$$

$$C_g = \frac{C_{aer}}{G}\ ,\ C_{aer} = \frac{P_{aer}}{\Omega_{tur}} \tag{2}$$

$$\Omega_{mec} = G\Omega_{tur} \tag{3}$$

The aerodynamic power is:

$$P_{aer} = C_p(\lambda;\beta)\frac{\rho}{2}sv^3 \tag{4}$$

And the coefficient of power C_p is [9], [10]:

$$C_p = 0.5 - 0.00167(\beta-2)\,sin\left[\frac{\pi(\lambda+0.1)}{18.5-0.3(\beta-2)}\right] - 0.00184(\lambda-3)(\beta-2) \tag{5}$$

3.2. Modeling of DFIG

In the Park model the DFIG electrical equations are [11]-[13].

$$\begin{cases} v_{ds} = R_s i_{ds} + \frac{d}{dt}\phi_{ds} - \omega_s\phi_{qs} \\ v_{qs} = R_s i_{qs} + \frac{d}{dt}\phi_{qs} + \omega_s\phi_{ds} \\ v_{dr} = R_r i_{dr} + \frac{d}{dt}\phi_{dr} - (\omega_s - \omega_r)\phi_{qr} \\ v_{qr} = R_r i_{qr} + \frac{d}{dt}\phi_{qr} + (\omega_s - \omega_r)\phi_{dr} \end{cases} \tag{6}$$

and:

$$\begin{cases} \phi_{ds} = L_s i_{ds} + M i_{dr} \\ \phi_{qs} = L_s i_{qs} + M i_{qr} \\ \phi_{dr} = L_r i_{dr} + M i_{ds} \\ \phi_{qr} = L_r i_{qr} + M i_{qs} \end{cases} \tag{7}$$

The electromagnetic torque equation:

$$C_{em} = p\frac{M}{L_s}\left(\phi_{qs}i_{dr} - \phi_{ds}i_{qr}\right) \tag{8}$$

4. CONTROL STRATEGY

In the two-phase reference, the active and reactive stator powers of the DFIG are defined [8], [14]:

$$\begin{cases} P_s = V_{ds}i_{ds} + V_{qs}i_{qs} \\ Q_s = V_{qs}i_{ds} - V_{ds}i_{qs} \end{cases} \tag{9}$$

Based on the orientation of the stator flux, on d-axis:

$$\phi_{qs} = 0\ ,\ \phi_{ds} = \phi_s \tag{10}$$

and:

$$V_{qs} = V_s \ , \ V_{ds} = 0 \tag{11}$$

From (9) becomes:

$$\begin{cases} P_s = V_{qs} i_{qs} \\ Q_s = V_{qs} i_{ds} \end{cases} \tag{12}$$

By combining (6), (7) and (12), we have:

$$\begin{cases} P_s = -V_s \frac{M}{L_s} i_{qr} \\ Q_s = -V_s \frac{M}{L_s} i_{dr} + \frac{V_s \phi_s}{L_s} \end{cases} \tag{13}$$

By substituting (7) in (6) and using (10), the rotor voltage is:

$$\begin{cases} v_{dr} = R_r i_{dr} + \left(L_r - \frac{M^2}{L_s}\right) \frac{di_{dr}}{dt} - g\left(L_r - \frac{M^2}{L_s}\right) \omega_s i_{qr} \\ v_{qr} = R_r i_{qr} + \left(L_r - \frac{M^2}{L_s}\right) \frac{di_{qr}}{dt} + g\left(L_r - \frac{M^2}{L_s}\right) \omega_s i_{dr} + g\frac{MV_s}{L_s} \end{cases} \tag{14}$$

4.1. Sliding mode control

Variable structure control with sliding mode is a nonlinear robust control approach. It provides dynamic behavior with an invariance property to uncertainties; it is simple and robust to internal or external disturbances. The sliding mode control consists of three phases:
Firstly: the choice of the surface sliding mode: using of the surface form proposed by Slotine [15], [16]:

$$\begin{cases} S(X) = \left(\frac{d}{dt} + \lambda_c\right)^{n-1} e \\ e = X^d - X \end{cases} \tag{15}$$

with:

$$\begin{cases} X = \left[x, \dot{x}, \ldots, x^{n-1}\right]^T \\ X^d = \left[x^d, \dot{x}^d, \ddot{x}^d, \ldots\right]^T \end{cases} \tag{16}$$

where e is error on the magnitude to be adjusted, λ is positive coefficient, n is the system order, X^d is desired magnitude, and X is variable of state of the magnitude ordered.
Secondly: ensure the convergence conditions and stability system; this is possible by the use of the Lyapunov stability criterion:

$$\left(S(X)\right)\left(\dot{S}(X)\right) \leq 0 \tag{17}$$

Thirdly: the design of the law control which can be defined by [17]:

$$u = u^{eq} + u^n \tag{18}$$

The control law is constructed in such a way that the system reaches the sliding surface and remains there forever. Where u^{eq} is the equivalent control and u^n is the switching term.

5. MODELING OF THE PHOTOVOLTAIC ENERGY CONVERSION SYSTEM

5.1. Modeling a real cell

The PV cell is described by a single diode model, as shown in Figure 2. The photovoltaic panel is modeled by a current source and two resistors, the first is in series and the second is in parallel. These resistors present losses due to the connections of conductors and semiconductors.

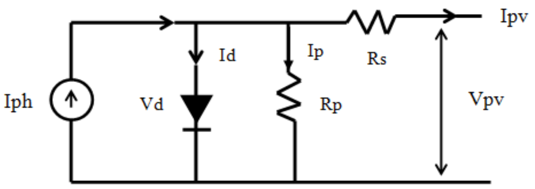

Figure 2. Photovoltaic cell [18], [19]

According to Kirchhoff's current law, the current equation of photovoltaic generator is [20]:

$$I_{pv} = I_{ph} - I_d - I_p \tag{19}$$

and:

$$\begin{cases} I_{pv} = I_{ph} - I_d \\ \quad = I_{ph} - I_0 \times \left(exp\left(\frac{e(V_{pv}+I_{pv}R_s)}{mKT_c}\right) - 1\right) - \frac{V_{pv}+I_{pv}R_s}{R_p} \end{cases} \tag{20}$$

$$I_0 = 1.5\times10^5\, exp\left(\frac{-E_g}{KT_c}\right)$$

Where I_o is saturation current of the unlit junction; e is the electron charge; K is Boltzmann's constant; T_c is the photovoltaic junction temperature; m is ideality factor of the junction; V_{pv} is voltage across the cell; R_s is series resistance; and R_p is shunt resistor.

5.2. Bus chopper booster

The boost converter is used to convert a low input voltage into a high output voltage [21], [22]. It consists of a continuous source voltage, inductance L, a switch S, a diode, and two capacitors *C1* and *C2*. The close time (αTs) and the open time ((1-α)Ts) is switched by the transistor of chopper at a constant frequency fs where: i) T_s is the switching period (T_s=1/f_s) and α is the cyclic ratio of the switch ($\alpha \in [0, 1]$). After applying Kirchhoff's laws on Figure 3, the equation systems according to Figure 4 are as (21):
In the 1st period αT_s:

$$\begin{cases} i_{c_1}(t) = c_1 \dfrac{dv_i(t)}{dt} = i_t(t) - i_L(t) \\ i_{c_2}(t) = c_2 \dfrac{dv_0(t)}{dt} = -i_0(t) \\ v_L(t) = L\dfrac{di_L}{dt} = v_i(t) - R_L i_L \end{cases} \tag{21}$$

In the 2nd period *(1-α) Ts*:

$$\begin{cases} i_{c_1}(t) = c_1 \dfrac{dv_i(t)}{dt} = i_i(t) - i_L(t) \\ i_{c_2}(t) = c_2 \dfrac{dv_0(t)}{dt} = i_L(t) - i_0(t) \\ v_L(t) = L\dfrac{di_L}{dt} = v_i(t) - v_0(t) - R_L i_L \end{cases} \tag{22}$$

So, in the T_s period, we have:

$$\frac{dx}{dt}T_s = \frac{dx}{dt_{(\alpha T_s)}}\alpha T_s + \frac{dx}{dt_{((1-\alpha)T_s)}}(1-\alpha)T_s \tag{23}$$

Applying the relation (23) to the system of (21) and to (22), the equations of system in T_s period can be:

$$\begin{cases} c_1 \dfrac{dv_i}{dt} T_s = \alpha T_s \left(i_i - i_L\right) + \left(1-\alpha\right) T_s \left(i_i - i_L\right) \\ c_2 \dfrac{dv_0}{dt} T_s = -\alpha T_s i_0 + \left(1-\alpha\right) T_s \left(i_L - i_0\right) \\ L \dfrac{di_L}{dt} T_s = \alpha T_s \left(v_i - R_L i_L\right) + \left(1-\alpha\right) T_s \left(v_i - v_0 - R_L i_L\right) \end{cases} \tag{24}$$

By arranging the terms of the preceding system of (24), the dynamic modeling of the boost converter is given by:

$$\begin{cases} i_L = i_i - c_1 \dfrac{dv_i(t)}{dt} \\ i_0 = \left(1-\alpha\right) i_L - c_2 \dfrac{dv_0(t)}{dt} \\ v_i = L \dfrac{di_L}{dt} + \left(1-\alpha\right) v_0 + R_L i_L \end{cases} \tag{25}$$

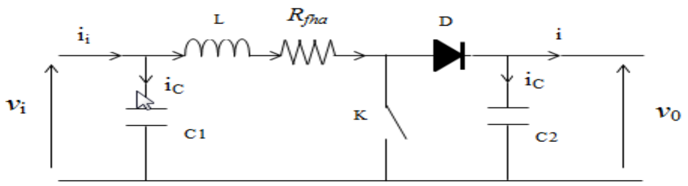

Figure 3. Boost converter

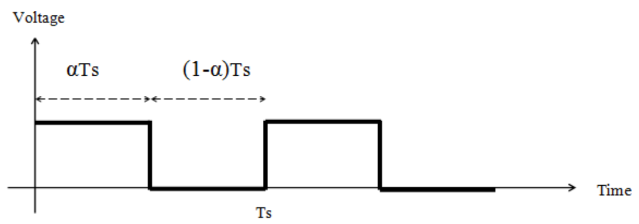

Figure 4. Close and open of switching periods

5.3. Chopper control

To control the power of the photovoltaic generator photovoltaic generator (PVG), it is necessary to adjust PVG voltage v_{pv}. This adjustment is possible by the control of cyclic ratio chopper (α) and the chopper filter current i_{fhac} [23]. To extract the PVG control law, it is necessary to study the two operating phases of the switch S:

– Close operating phases of S_{hac} $(0<t<\alpha T_s)$:

$$\frac{di_{fhac}}{dt} = \frac{1}{L_{fhac}}\left(v_{pv} - R_{fhac} i_{fhac}\right) \tag{26}$$

– Open operating phases of S_{hac} $(\alpha T_s<t<T_s)$:

$$\frac{di_{fhac}}{dt} = \frac{1}{L_{fhac}}\left(v_{pv} - v_{dc} - R_{fhac} i_{fhac}\right) \tag{27}$$

From (23), the variation of the i_{fhac} is being a linear form, so the derivative of the variable i_{fhac} can be defined according to (23) in αT_s and $(1-\alpha)T_s$ periods:

$$\frac{di_{fhac}}{dt}T_s = \frac{di_{fhac}}{dt_{(\alpha T_S)}}\alpha T_s + \frac{di_{fhac}}{dt_{((1-\alpha)T_S)}}(1-\alpha)T_s \tag{28}$$

Substituting (26) and (27) in (28), the equations of system in T_s period can be:

$$\frac{di_{fhac}}{dt} = \frac{1}{L_{fhac}}\left(v_{pv} - (1-\alpha)v_{dc} - R_{fhac}i_{fhac}\right) \tag{29}$$

So, the cyclic ratio chopper (α) control is given by:

$$\alpha = \frac{v_{fhac}+v_{dc}-v_{pv}}{v_{dc}} \tag{30}$$

6. MODELING OF THE BATTERY

Interruptions due to day/night alternation and the absence of the sunshine are considered disadvantages. The use of a group of batteries becomes necessary for the continuity of the supply.

6.1. Model of the battery

The battery electrical model is [24]:

$$V_{batt} = E_0 - (R_s \times i) - V_{cbatt} \tag{31}$$

The state of charge (SOC) of the battery is also defined by:

$$SOC = 1 - \frac{Q_d}{C_{batt}} \tag{32}$$

where C_{batt} is nominal capacity of battery, and Q_d is the amount of charge missing compared to C_{batt}.
The capacity is modeled by:

$$Q_{batt} = I \times t_{batt} \tag{33}$$

$$C = \frac{Q_{batt}}{V} \tag{34}$$

where Q_{batt} is amount of electrical charge in Coulomb, I is current through the capacity, t is operating time, C is value of the Farad capacity, and V is potential difference corresponding to a range of SOC ranging from 0% to 100%. For n_b cells in series, the battery voltage is [24]:

$$V_{batt} = n_b E_b + n_b R_i I_{batt} \tag{35}$$

where V_{batt} is voltage of battery, I_{batt} is current battery, E_b is electromotive force according to the SOC, and R_i is internal resistance of an element.

6.2. Capacity model

The capacity model is obtained from the discharge current expression in 10 h (I_{10}). It corresponds to the operating mode of the discharge capacity in 10 h (C_{10}) [24]:

$$C_{batt} = C_{10}\frac{1.67}{1+0.67\left(\frac{I_{battmoy}}{I_{10}}\right)^{0.9}}\left(1+0.005\Delta T\right) \tag{36}$$

6.3. Equation of the voltage in discharge of battery

The expression of the battery voltage is established from (35) and (36) which allows us to give a linked structure of the internal elements of the battery according to the electromotive force, the internal resistance and the influence of the parameters [25].

$$V_d = n_b\big(0.085 - 0.12(1 - SOC)\big) - n_b \frac{|I_{batt}|}{C_{10}}\left[\frac{4}{1+|I_{batt}|^{1.3}} + \frac{0.27}{(SOC)^{1.5}} + 0.02\right](1 - 0.007\Delta T) \quad (37)$$

6.4. Equation of the voltage in the charge of battery

Indeed, the charge equation of the battery voltage has the same structure as (37) which shows the influence of the electromotive force and the internal resistance [25].

$$V_c = n_b(2 + 0.16SOC) + n_b \frac{|I_{batt}|}{C_{10}}\left[\frac{6}{1+|I_{batt}|^{0.86}} + \frac{0.48}{(1-SOC)^{1.2}} + 0.036\right](1 - 0.025\Delta T) \quad (38)$$

7. STRATEGY OF THE MANAGEMENT OF THE SYSTEM STUDIED BY A SUPERVISOR

To manage the generated electrical energy and guarantee the continuity of the service (no power failure), we need a supervisor, which optimizes the use of the energy produced by the manual commutation or the automatic auxiliary power supply, by opening or closing the contacts (C1-C4) as indicated in Figure 1.
At first: the supervisor checks the power status of the batteries, as they must be in a fully charged mode.
Secondly: the supervisor measures the value of powers in the PV system (P_{pv}) and rotor (P_r), and the value of Continuous tension in the system and battery storage.
Thirdly: the supervisor compares the power required by the rotor and available at the batteries and the PV system level, where the appropriate supply source is determined according to the following cases:

– 1st case: if: $P_{pv} > P_r$: the supervisor must assure the supply of the DFIG rotor with the PV generator by closing the contact C1 and keeping the battery group in the charging position by closing the contact C2 and opening the contact C3 as shows in Figure 1.
– 2nd case: if: $0 < P_{pv} < P_r$: the supervisor must assure the supply of the DFIG rotor with two sources (generator PV, battery group) for the energy compensation, by closing the contacts C1 and C3, and opening the contacts C2 and C4 as shows in Figure 1.
– 3rd case: if: $P_{pv}=0$: the supervisor must assure the supply of the DFIG rotor with the group battery (in the night), by closing the contact C3 and opening the contacts C1, C2 and C4 as shows in Figure 1. Figure 5 presents the supervisor algorithm system.

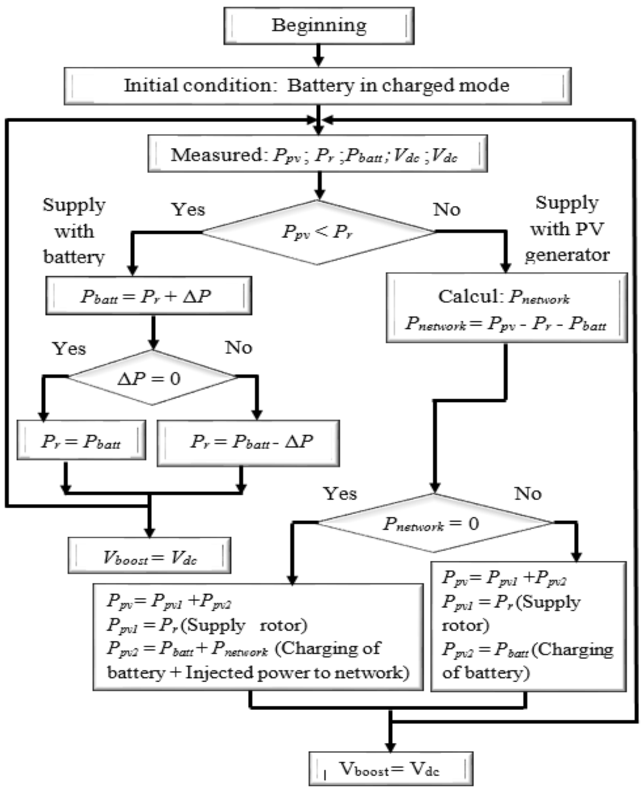

Figure 5. Supervisor algorithm system

8. RESULTS OF SIMULATIONS

In this section, the simulation of DC voltage adaptation system, the currents and voltages rotor, the sliding mode control technique of powers DFIG generating is described in MATLAB/Simulink environment. Then, the photovoltaic system simulation is given to find the maximum power produced in PV system. Finally, to show the reliability of the proposed control strategy, the different deficiency cases is simulated. To ensure a good power supply to the inverter and the battery bank, the switching voltage (vdc) was adapted to the value of 336 V, as shown in Figure 6. At the interval t [0, 0.04], there is a transition step due to start-up. From the instant t=0.04 s, the system is stabilized at the value of vdc=336 V.

The battery bank provides a continuous voltage V_{dcbatt} =336 V to supply the rotor DFIG and facilitate the coupling with the system, as shown in Figure 7. The simulation of the system discovers a fast and acceptable variation of the voltage V_{rabc} and the current I_{rabc} as shown in Figure 8 and Figure 9. The sliding mode control technique is used to control the DFIG stator powers (Ps and Qs).

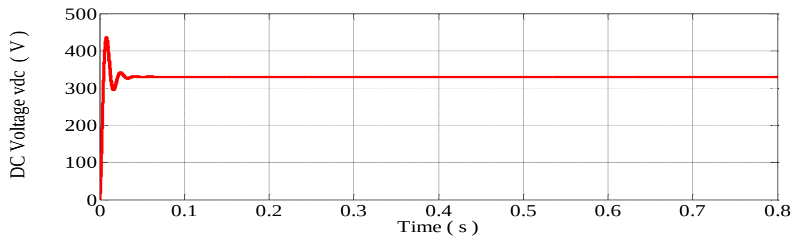

Figure 6. Voltage v_{dc} regulated with chopper

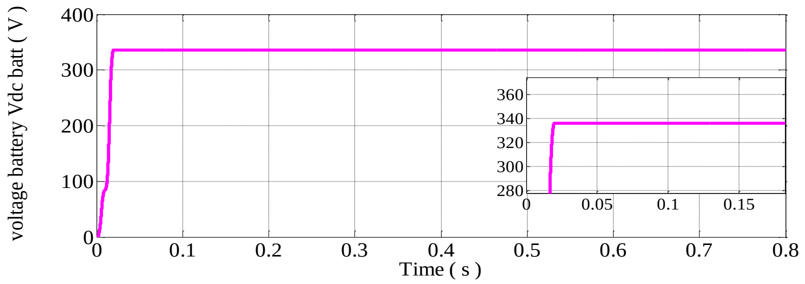

Figure 7. Voltage v_{dcbatt} regulated with chopper auxiliary battery

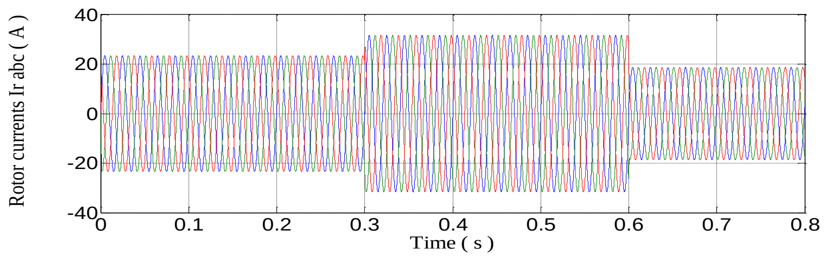

Figure 8. Rotor currents feeding the DFIG

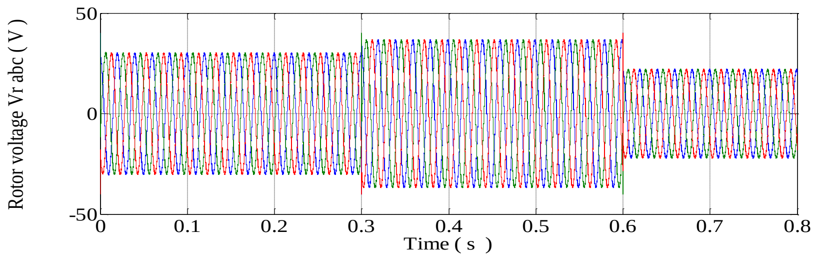

Figure 9. Rotor voltage feeding the DFIG

The comparison in the cases of the PI and the sliding mode control (SMC) controllers is used to show the robustness of the control system of the active and reactive powers. Najafi-Shad *et al*. [6] studied the control of the hybrid system by means of a PI controller, which gave satisfactory results. But the sliding mode control had previously proven its efficacy in the independent classical systems (wind system, PV system). So, we used the control by sliding mode, to proven his efficacy by the comparison between the controller PI and sliding mode where we got better results: a very fast response time, good robustness, very fast adaptation to the disturbance of the system parameters (wind, lighting, and reference parameters) as shows in Figures 10 and 11.

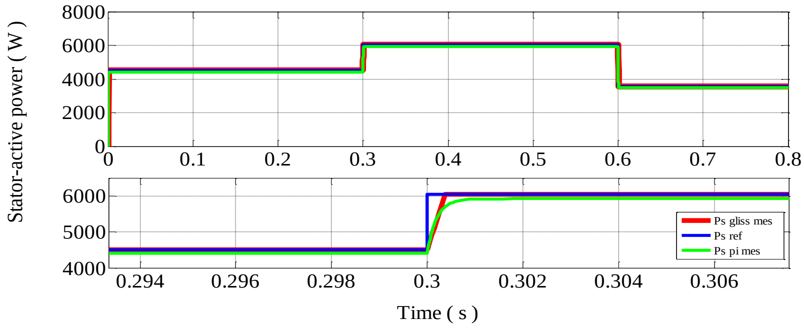

Figure 10. Regulation of active powers by controller PI and SMC

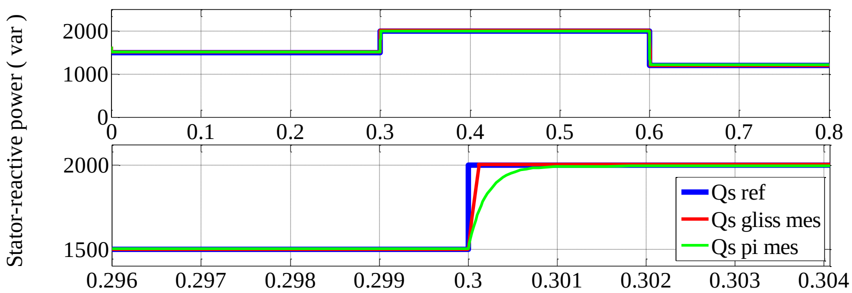

Figure 11. Regulation of reactive powers by controller PI and SMC

Figures 10 and 11 show that the control of the active and reactive powers by SMC technique is very fast compared to the PI technique with more precision. So, the control by SMC is robust compared to the control by PI. For different states, it does can follow the scenario declared in the management strategy of the studied system. In the case of an ordinary state (maximum lighting, no fault in the photovoltaic system), the photovoltaic system generates a stable power of a value 6.8 kW (Figure 12). The first part of this power, which does not exceed 700 W at full load, is consumed by the DFIG rotor (Figure 13). The second part P_{rest} is variable depending on the consumption of the rotor, as shown in Figure 14. It is used to charge the group of batteries in case it is discharged. The rest is injected into the network. In the case of a problem in the photovoltaic system (system failure, absence of sun, and low lighting), it is necessary to compensate for the lack of power supply Pr using the group of batteries with manual or automatic switching.

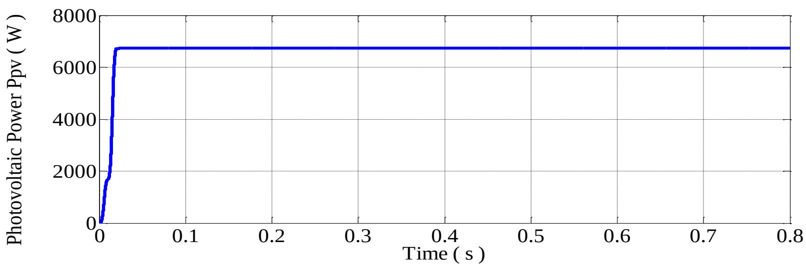

Figure 12. PV generated power

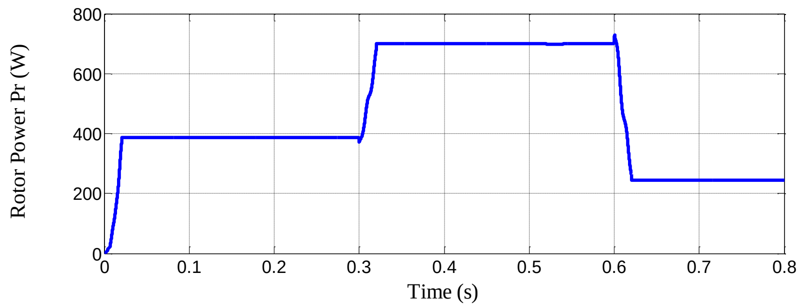

Figure 13. Rotor consumed power

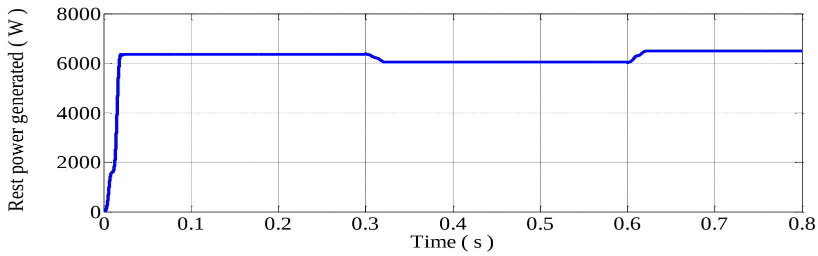

Figure 14. The rest power generated by the PV

Figures 15-17 respectively shows the variation of the powers (P_{pv}, P_r, P_{rest}) and the switching between the DC voltages (v_{dc}, V_{dcbatt}) for the supply of the inverter under transient conditions. At the period t=[0 0.1] s, the power P_{pv}=6.75 kW is greater than the power demanded by the rotor P_r=0.39 kW (1st case of the control strategy), so the power benefit of P_{rest}=6.36 kW (Figure 16(a)) is injected into the network. During this period, the system is supplied by the PV group with a voltage of v_{dc}=336 V. The battery group is not used ($V_{dc\ batt}$=0 V), as shown in Figure 17 (no compensation by the battery group). From t=0.1 s to t=0.2 s, the value of the power P_{pv} is 0.145 kW, it is lower than the power required by the rotor (P_r=0.39 kW) because of lack of power due to the lack of lighting (G=70 w/m^2), as shown in Figures 15 and Figure 16(b). In this case, the supervisor looks for the equilibrium point, the lack of power is compensated using the battery group (P_{batt}=0.245 kW) with the voltage $V_{dc\ batt}$=336 V, as shown in Figure 17. From t=0.24 s to t=0.4 s, there is an increase of the lighting, then of the photovoltaic power P_{pv}=6.75 kW (first case of the control strategy). From t=0.4 s to t=0.52 s, the power genetated by photovoltaic generator is P_{pv}=0 kW as shown in Figure 15 (3rd case of the control strategy) so we have a lack of power P_{rest}=-700 kW (Figure 16(c)). It is due to a system failure or a problem at the recovery level (v_{dc}=0V) as shown in Figure 17. The supervisor must be powered by the capacitor bank ($V_{dc\ batt}$=336 V). Finally, after the moment t=0.62 s (Figure 16(d)), the system returns to the normal state (1st case of the control strategy).

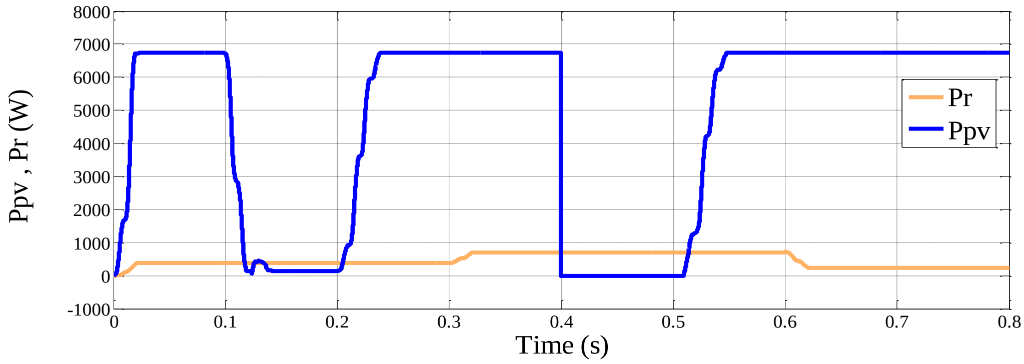

Figure 15. The appearance of the variation of the powers (P_{pv}, P_r) in the transitory regime

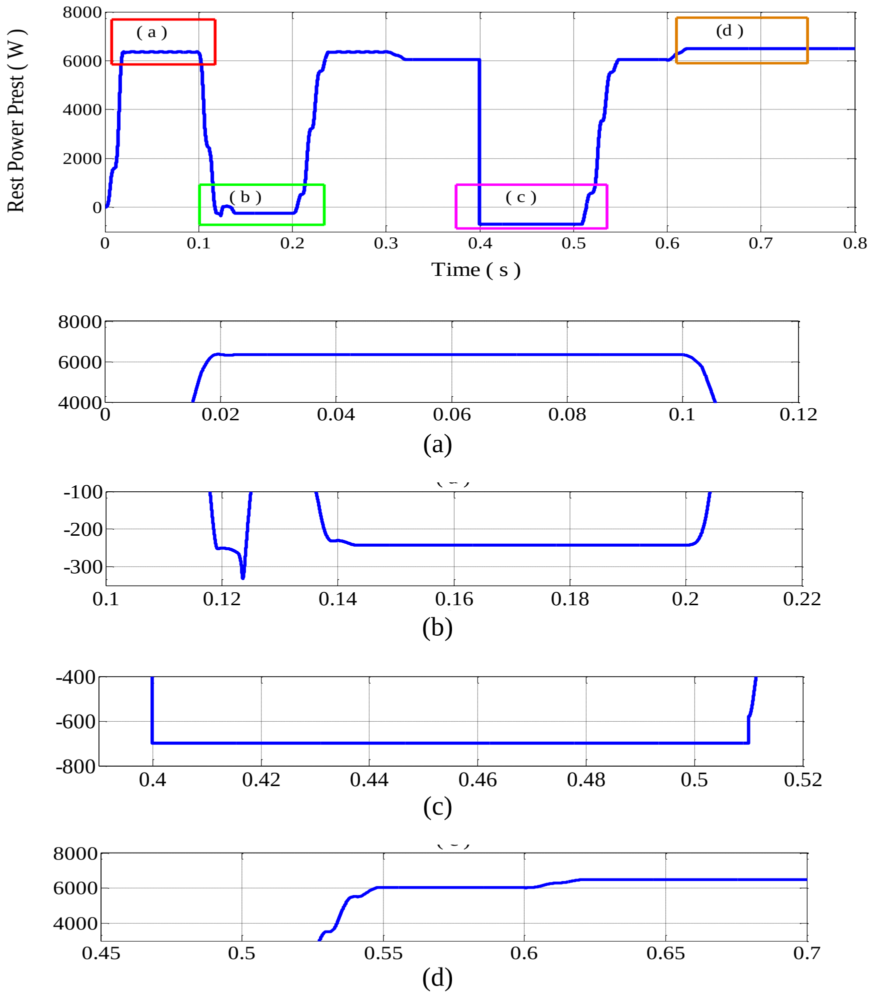

Figure 16. The appearance of the variation of the powers P_{rest} in the transitory regime (a) the injected power into the network (beneficiary power), (b) lack of power due to lack of lighting, (c) lack of power due to the failure system or problem on the PV generator, and (d) the injected power into the network after the return to the normal state

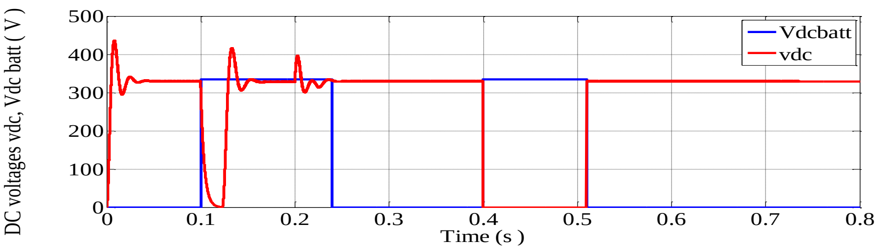

Figure 17. The switching between the DC voltages (v_{dc}, $V_{dc\ batt}$) in the transient regime (fault assumption)

9. CONCLUSION

In this article, has been confirmed the reliability, cost-effectiveness and fast reactions against fugitive interruptions in a hybrid electric power generation system with three generation sources (wind turbine, photovoltaic, and battery capacitors). The primary source is the wind turbine conversion chain; it is equipped with a DFIG. The active and reactive powers of DFIG are controlled using two types of control methods: conventional method (PI) and sliding mode control method. The sliding mode controller has high accuracy and robustness compared to the PI controller. The DFIG rotor supply is provided by a photovoltaic conversion chain and by the battery group. The photovoltaic conversion chain is equipped with a controller to track the maximum power point using the P&O bserved direct search method.

In the normal case, the additional energy generated by the photovoltaic system is transmitted to the grid and to the charge of the battery pack. In the case of a problem with the photovoltaic system (system failure or lack of sunlight), the supervisor must ensure the supply of the DFIG rotor by managing the switching between the two rotor power sources (PV/battery) by following a power management strategy. Finally, simulations are done in the MATLAB-Simulink environment; the results found prove the effectiveness of the system proposed against all incidents on the hybrid system of electricity production.

REFERENCES

[1] M. El Azzaoui, H. Mahmoudi, and K. Boudaraia, "Backstepping Control of Wind and Photovoltaic Hybrid Renewable Energy System," *International Journal of Power Electronics and Drive Systems (IJPEDS),* vol. 7, no. 3, pp. 677–686, Sep. 2016, doi: 10.11591/ijpeds.v7.i3.pp677-687.

[2] H. Laabidi, H. Jouini, and A Mami, "Sliding mode control for PV-wind hybrid system connected to grid," *International Conference on Green Energy & Environmental Engineering (GEEE-2018) Proceedings of Engineering and Technology–PET,* vol. 37, pp. 39-44, 2018, [Online]. Available: http://ipco-co.com/PET_Journal/GEEE-2018/51.pdf.

[3] M. Kendzi, A. Aissaoui, M. Abid, and A. Tahour, "Control of the photoelectric generator for used in feeding of the independent wind turbine system," *International Journal of Power Electronics and Drive System (IJPEDS),* vol. 10, no. 3, pp. 1613-1627, Sep. 2019, doi: 10.11591/ijpeds.v10.i3.pp1613-1627.

[4] L. Gomez, A. Grilo, M. Salles, and A. S. Filho, "Combined Control of DFIG-Based Wind Turbine and Battery Energy Storage System for Frequency Response in Microgrids," *Energies,* vol. 13, no. 4, p. 894, 2020, doi: 10.3390/en13040894.

[5] B. Toual, L. Mokrani, A. Kouzou, and M. Machmoum, "Power Quality and Capability Enhancement of a Wind-Solar-Battery Hybrid Power System," *Periodica Polytechnica Electrical Engineering and Computer Science,* vol. 64, no. 2, pp. 115-132, 2020, doi: 10.3311/PPee.14437.

[6] S. Najafi-Shad, S. Barakati, and A. Yazdani, "An effective hybrid wind-photovoltaic system including battery energy storage with reducing control loops and omitting PV converter," *Journal of Energy Storage,* vol. 27, p. 101088, 2020, doi: 10.1016/j.est.2019.101088.

[7] P. Ponce, H. Ponce, and A. Molina, "Doubly fed induction generator (DFIG) wind turbine controlled by artificial organic networks, " *Soft Computing, Methodologies and Application, Springer,* vol. 22, no. 9, pp. 2867–2879, 2018, doi: 10.1007/s00500-017-2537-3.

[8] F. Mansouri, B. Mokhtar, and M. Benyounes, "Sliding mode performance control applied to a DFIG system for a wind energy production, " *International Journal of Electrical and Computer Engineering (IJECE),* vol. 10, no. 6, pp. 6139-6152, 2020, doi: 10.11591/ijece.v10i6.pp6139-6152.

[9] T. Douadi, Y. Harbouche, R. Abdessemed, and I. Bakhti, "Improvement performances of active and reactive power control applied to DFIG for variable speed wind turbine using sliding mode control and FOC, " *International Journal of Engineering,* vol. 31, no. 10, pp.1689-1697, 2018, doi: 10.5829/ije.2018.31.10a.11.

[10] M. Kendzi and A. Aissaoui, "Comparison Between the MIT Rule and Fuzzy Logic Controller to Adapting the Power Generated by a Doubly Fed Induction Generator Integrated in a Wind System," *2022 10th International Conference on Smart Grid (icSmartGrid),* 2022, pp. 231-235, doi: 10.1109/icSmartGrid55722.2022.9848520.

[11] K. Belgacem, A. Mezouar, and N. Essounbouli, "Design and analysis of adaptive sliding mode with exponential reaching law control for double-fed induction generator based wind turbine," *International Journal of Power Electronics and Drive System (IJPEDS),* vol. 9, no. 4, pp. 1534-1544, 2018, doi: 10.11591/ijpeds.v9.i4.pp1534-1544.

[12] A. Djoudia, S. Bacha, H. Iman-Eini, and T. Rekioua, "Sliding mode control of DFIG powers in the case of unknown flux and rotor currents with reduced switching frequency, " *International Journal of Electrical Power & Energy Systems,* vol. 96, pp. 347-356, 2018, doi: 10.1016/j.ijepes.2017.10.009.

[13] O. Boughazi, A. Bouiri, and Ch. Benoudjafer, "A robust new full control strategy without FOANR based on substitution method against nonlinear DFIG model for wind application, " *International Journal of Power Electronics and Drive System (IJPEDS),* vol. 13, no. 3, pp. 1694-1701, 2022, doi: 10.11591/ijpeds.v13.i3.pp1694-1701.

[14] A. Guediri and A. Guediri, "Modeling and comparison of fuzzy-PI and genetic control algorithms for active and reactive power flow between the stator (DFIG) and the grid, " *Engineering, Technology & Applied Science Research,* vol. 12, no. 3, pp. 8640-8645, 2022.

[15] O. Zouaid and L. Nezli, "Control with sliding mode of a fivephase series-connected two-asynchronous motor drive," *International Journal of Energetica (IJECA),* vol. 3, no. 1. pp. 18-23, 2018, doi: 10.47238/ijeca.v3i1.61.

[16] O. Moussa, R. Abdessemed, S. Benaggoune, and H. Benguesmia, "Comparative study between sliding mode control and the vectorial control of a brushless doubly fed induction generator, " *International Journal of Energetica (IJECA),* vol. 3, no. 2, pp. 22-28, 2018, doi: 10.47238/ijeca.v3i2.74.

[17] A. Herizi, and R. Rouabhi, "Hybrid Control Using Sliding Mode Control with Interval Type-2 Fuzzy Controller of a Doubly Fed Induction Generator for Wind Energy Conversion, " *International Journal of Intelligent Engineering and Systems*, vol. 15, no. 1, 2022, doi: 10.22266/ijies2022.0228.50.

[18] S. A. Ardjoun, "*Control of a renewable energy system multisource connected to the electrical network*," Ph.D. Electrical Engineering, University Djillali Liabes of Sidi-Bel-Abbes., Algeria, 2016.

[19] M. Wang, H. Li, H, and S. Wang, "Photovoltaic cell MPPT simulation system based on hybrid algorithm," *Chemical Engineering Transactions,* vol. 71, pp. 169-174, 2018, doi: 10.3303/CET1871029.

[20] R. Moltames and M. Boroushaki, "Sensitivity analysis and parameters calculation of PV solar panel based on empirical data and two-diode circuit model, " *Energy Equipment and Systems,* vol. 6, no. 3, pp. 235-246, 2018, doi: 10.22059/EES.2018.32225.

[21] N. Agarwal, "Design and Simulink of intelligent solar energy improvement with PV module, " *International Journal of Information and Computation Technology,* vol. 4, no. 6, pp. 619–628, 2014.

[22] S. Umashankar, K. P. Aparna, R. Priya, and S. Suryanarayanan, "Modeling and simulation of a PV system using DC-DC converter, " *International Journal of Latest Research in Engineering and Technology, (IJLRET),* vol. 1, no. 2, pp. 2454-5031, 2015, [Online]: Available: http://www.ijlret.com/Papers/Vol-1-issue-2/2- A037%20(Final%20Version).pdf.

[23] M. Kendzi, A. Aissaoui, A. Hasnia, and A. Tahour, "Control of the Energy Produced by Photovoltaic System Using the Fuzzy PI Controller, " *Springer Nature Switzerland AG 2020,* pp. 132–142, 2020, doi: 10.1007/978-3-030-37207-1_14.

[24] A. Trindade and L. Cordeiro, "Automated verification of stand-alone solar photovoltaic systems," *arXiv preprint arXiv:1811.09438*, 2018, doi: 10.1016/j.solener.2019.09.093.

[25] N. Achaibou, M. Haddadi, and A. Malek, "Modeling of lead acid batteries in PV systems, " *Energy Procedia,* vol. 18, pp. 538–544, 2012, doi: 10.1016/j.egypro.2012.05.065.

BIOGRAPHIES OF AUTHORS

Kendzi Mohammed doctor en Génie Electrique at the University of TAHRI Mohammed, Bechar, (Algeria). He was born in 1984 in Naama, Algeria. He received his BS degree in 2003, the MS degree in 2012, the Ph.D degree in 2020 from Department of Electrical Engineering, University TAHRI Mohammed, Bechar, (Algeria). His current research interest includes power electronics, control of electrical machines, artificial intelligence, and renewable energies. He can be contacted at email: kendzimohammed@gmail.com.

Aissaoui Abdelghani is a full Professor of electrical engineering at University of Bechar (Algeria). He was born in 1969 in Naama, Algeria. He received his BS degree in 1993, the MS degree in 1997, the Ph.D degree in 2007 from the Electrical Engineering Institute of Djilali Liabes University of Sidi Bel Abbes (Algeria). He is an active member of IRECOM Laboratory and IEEE senior member. His current research interest includes power electronics, control of electrical machines, artificial intelligence, and renewable energies. He can be contacted at email: irecom_aissaoui@yahoo.fr.

Younes Dris was born in Ghazaouet, Algeria, on October 24, 1991. He received his master's degree in electrical engineering from the University of Tlemcen (Algeria) in 2015. He obtained his Ph.D in 2009 at Tlemcen University, Algeria. His research interests concern: power electronics, electrical machines, photovoltaic systems, storage systems, and renewable energies. He can be contacted at email: younes.dris@univ-tlemcen.dz.

Bouiri Abdesselam he is a member of Smart Grid and Renewable Energy Laboratory (SGRE), since 2018. He received B.Eng. and M.Eng degree in electrical engineering and electric network from Tahri Mohammed Bechar University, (Algeria), in 2016 and 2018 respectively. He received Ph.D degree in advanced power electronics from same university in 2022. His main research activity is focused on electrical mechines, nonlinear control, wind energy, and power electronics applications. He can be contacted at email: abdou.dwidi@gmail.com.

Haddar Mabrouk was born in El-eulma, Setif, Algeria, in 1989. He received his Bachelor's degree in "Electronics" and Master's degree in "Industrial Electronics" from Ferhat Abbes University, Setif, Algeria in 2009 and 2012, respectively. He received his Ph.D degree in advanced power electronics from Tahri Mohammed University, Bechar, Algeria in 2022. His current scientific interest includes power converters, advanced control and renewable energy conversion. Currently, he is a member of the Smart Grids AND Renewable Energies (SGRE) Laboratory, Bechar, Algeria. He can be contacted at email: haddar.mabrouk@univ-bechar.dz.